The Mutational Landscape of Head and Neck Squamous Cell Carcinoma

Nicolas Stransky *et al.*

Science **333**, 1157 (2011);
DOI: 10.1126/science.1208130

Science (print ISSN 0036-8075; online ISSN 1095-9203) is published weekly, except the last week in December, by the American Association for the Advancement of Science, 1200 New York Avenue NW, Washington, DC 20005.

Acknowledgments: We thank our patients for their courage and generosity. We thank N. Silliman, J. Ptak, M. Whalen, L. Dobbyn, J. Schaeffer, X. Li, O. Folawiyo, and Z. Khan for expert technical assistance. This work was supported by the National Institutes of Health (NIH)/National Institute of Dental and Craniofacial Research grants RC2DE020957, and RC2DE020958; NIH grants CA121113, CA43460, CA57345, and CN43302; NIH Specialized Program of Research Excellence grants P50DE019032 and 5P50CA09700708; Cancer Prevention Research Institute of Texas grant RP100233; Cancer Center Support grant CA16672; AACR Stand Up To Cancer–Dream Team Translational Cancer Research grant; and the Virginia and D. K. Ludwig Fund for Cancer Research. Under agreements between the Johns Hopkins University, Genzyme, Exact Sciences, Inostics, Qiagen, Invitrogen, and Personal Genome Diagnostics, N.P., B.V., K.W.K., and V.E.V are entitled to a share of the royalties received by the university on sales of products related to genes and technologies described in this manuscript. N.P., B.V., K.W.K., and V.E.V are co-founders of Inostics and Personal Genome Diagnostics, are members of their Scientific Advisory Boards, and own Inostics and Personal Genome Diagnostics stock, which is subject to certain restrictions under Johns Hopkins University policy. J.C. is the Director of Research of the Milton J. Dance Head and Neck Endowment. The terms of these arrangements are managed by the Johns Hopkins University in accordance with its conflict-of-interest policies. C.B. is a recipient of T32 CA009574 NIH/National Cancer Institute National Research Service Award. C.R.P. is a TRIUMPH Fellow and supported by the GSK Translational Research Fellowship. This paper is based on a web database application provided by Research Information Technology Systems (RITS) www.rits.onc.jhmi.edu/.

Supporting Online Material
www.sciencemag.org/cgi/content/full/science.1206923/DC1
Materials and Methods
Figs. S1 to S6
Tables S1 to S8
References

13 April 2011; accepted July 5 2011
Published online 28 July 2011;
10.1126/science.1206923

The Mutational Landscape of Head and Neck Squamous Cell Carcinoma

Nicolas Stransky,[1]* Ann Marie Egloff,[2]* Aaron D. Tward,[1,3,4]* Aleksandar D. Kostic,[1,5] Kristian Cibulskis,[1] Andrey Sivachenko,[1] Gregory V. Kryukov,[1,5] Michael S. Lawrence,[1] Carrie Sougnez,[1] Aaron McKenna,[1] Erica Shefler,[1] Alex H. Ramos,[1] Petar Stojanov,[1] Scott L. Carter,[1] Douglas Voet,[1] Maria L. Cortés,[1] Daniel Auclair,[1] Michael F. Berger,[1] Gordon Saksena,[1] Candace Guiducci,[1] Robert C. Onofrio,[1] Melissa Parkin,[1] Marjorie Romkes,[6] Joel L. Weissfeld,[7] Raja R. Seethala,[8] Lin Wang,[8] Claudia Rangel-Escareño,[9] Juan Carlos Fernandez-Lopez,[9] Alfredo Hidalgo-Miranda,[9] Jorge Melendez-Zajgla,[9] Wendy Winckler,[1] Kristin Ardlie,[1] Stacey B. Gabriel,[1] Matthew Meyerson,[1,5,10,11] Eric S. Lander,[1,5,12] Gad Getz,[1] Todd R. Golub,[1,5,11,13,14]† Levi A. Garraway,[1,5,10,11]†‡ Jennifer R. Grandis[2,15]†‡

Head and neck squamous cell carcinoma (HNSCC) is a common, morbid, and frequently lethal malignancy. To uncover its mutational spectrum, we analyzed whole-exome sequencing data from 74 tumor-normal pairs. The majority exhibited a mutational profile consistent with tobacco exposure; human papillomavirus was detectable by sequencing DNA from infected tumors. In addition to identifying previously known HNSCC genes (*TP53*, *CDKN2A*, *PTEN*, *PIK3CA*, and *HRAS*), our analysis revealed many genes not previously implicated in this malignancy. At least 30% of cases harbored mutations in genes that regulate squamous differentiation (for example, *NOTCH1*, *IRF6*, and *TP63*), implicating its dysregulation as a major driver of HNSCC carcinogenesis. More generally, the results indicate the ability of large-scale sequencing to reveal fundamental tumorigenic mechanisms.

Head and neck squamous cell carcinoma (HNSCC) is the sixth most common non-skin cancer in the world, with an incidence of ~600,000 cases per year and a mortality rate of ~50% (*1*). The major risk factors for HNSCC are tobacco use, alcohol consumption, and infection with human papillomavirus (HPV) (*2*). Despite advances in our knowledge of its epidemiology and pathogenesis, the survival rates for many types of HNSCC have improved little over the past 40 years (*3*). As such, a deeper understanding of HNSCC pathogenesis is needed to promote the development of improved therapeutic approaches.

We performed solution-phase hybrid capture and whole-exome sequencing on paired DNA samples (tumors and matched whole blood) from 92 HNSCC patients. Most anatomic sites were represented (oral cavity, oropharynx, hypopharynx, larynx, and sinonasal cavity) (Fig. 1C and table S1). Of the patients profiled in this study, 89 and 79% reported a history of tobacco and alcohol use, respectively (table S1). Initially, 14% of all tumors and 53% of oropharyngeal tumors were found to be positive for HPV based on HPV-16 polymerase chain reaction (PCR)/in situ hybridization (Fig. 1 and table S1). Tumor copy-number analysis with the use of single-nucleotide polymorphism (SNP) arrays (fig. S1) replicated previous findings of frequent *CCND1* amplifications; *CDKN2A* deletions; and rarer *MYC*, *EGFR*, *ERBB2*, or *CCNE1* amplifications (*4*), indicating that the collection is genetically representative of HNSCC.

We achieved 150-fold mean sequence coverage of targeted exonic regions, with 87% of loci covered at >20-fold (figs. S2 and S3 and table S2). We excluded from further analysis 18 tumors in which initial analysis revealed extensive stromal admixture (figs. S3 and S4 and supplemental methods), leaving 74 samples for analysis. We also performed whole-genome sequencing (31-fold mean coverage) (table S3) on an oropharyngeal tumor and a hypopharyngeal tumor.

On average, we identified 130 coding mutations per tumor, 25% of which were synonymous (Fig. 1A). We queried 321 of these mutations by mass spectrometric genotyping and validated 288 (89.7%). However, the validation rate increased to 95.7% for mutations whose allelic fraction was >20% of total DNA, suggesting that the sensitivity of mass spectrometric genotyping may be reduced in the setting of increased stromal admixture.

The overall HNSCC mutation rate was comparable to other smoking-related malignancies such as small-cell lung cancer and lung adenocarcinoma (*5*, *6*). The mutation rate of HPV-positive tumors was approximately half of that found in HPV-negative HNSCC (mean = 2.28 mutations per megabase compared with 4.83 mutations per megabase; $P = 0.004$, rank sum test), consistent with epidemiologic studies suggestive of biological differences between HPV-positive and -negative disease. The two tumors that underwent whole-genome sequencing harbored 19 (HN_62469) and 111 (HN_62699) high-confidence somatic rearrangements, respectively (fig. S5 and tables S4 and S5).

Although base mutation rates varied widely (0.59 to 24 mutations per megabase; Fig. 1A), the average rate of guanosine-to-thymidine (G → T) transversions at non-CpG sites (12 ± 6%, standard deviation) was characteristic of tobacco exposure (Fig. 1B). Among patients who reported a smoking history, tumors with the highest fraction of G → T transversions showed a tendency toward increased overall mutation rates ($P = 0.02$, Spearman rank correlation) (Fig. 1, B and C). Thus, the G → T transversion frequency

[1]The Broad Institute of MIT and Harvard, Cambridge, MA 02142, USA. [2]Department of Otolaryngology, University of Pittsburgh and University of Pittsburgh Cancer Institute, Pittsburgh, PA 15213, USA. [3]Department of Otology and Laryngology, Harvard Medical School, Boston, MA 02114, USA. [4]Department of Otolaryngology, Massachusetts Eye and Ear Infirmary, Boston, MA 02114, USA. [5]Harvard Medical School, Boston, MA 02115, USA. [6]Department of Medicine, University of Pittsburgh and University of Pittsburgh Cancer Institute, Pittsburgh, PA 15261, USA. [7]Department of Epidemiology, University of Pittsburgh and University of Pittsburgh Cancer Institute, Pittsburgh, PA 15232, USA. [8]Department of Pathology, University of Pittsburgh and University of Pittsburgh Cancer Institute, Pittsburgh, PA 15213, USA. [9]Instituto Nacional de Medicina Genómica, Mexico City, 01900, Mexico. [10]Department of Medical Oncology, Dana-Farber Cancer Institute, Boston, MA 02115, USA. [11]Center for Cancer Genome Discovery, Dana-Farber Cancer Institute, Boston, MA 02115, USA. [12]Massachusetts Institute of Technology, Cambridge, MA 02142, USA. [13]Department of Pediatric Oncology, Dana-Farber Cancer Institute, Boston, MA 02115, USA. [14]Howard Hughes Medical Institute, Chevy Chase, MD 20815, USA. [15]Department of Pharmacology and Chemical Biology, University of Pittsburgh and University of Pittsburgh Cancer Institute, Pittsburgh, PA 15213, USA.

*These authors contributed equally to this work.
†These authors contributed equally to this work.
‡To whom correspondence should be addressed. E-mail: levi_garraway@dfci.harvard.edu (L.A.G.); grandisjr@upmc.edu (J.R.G.)

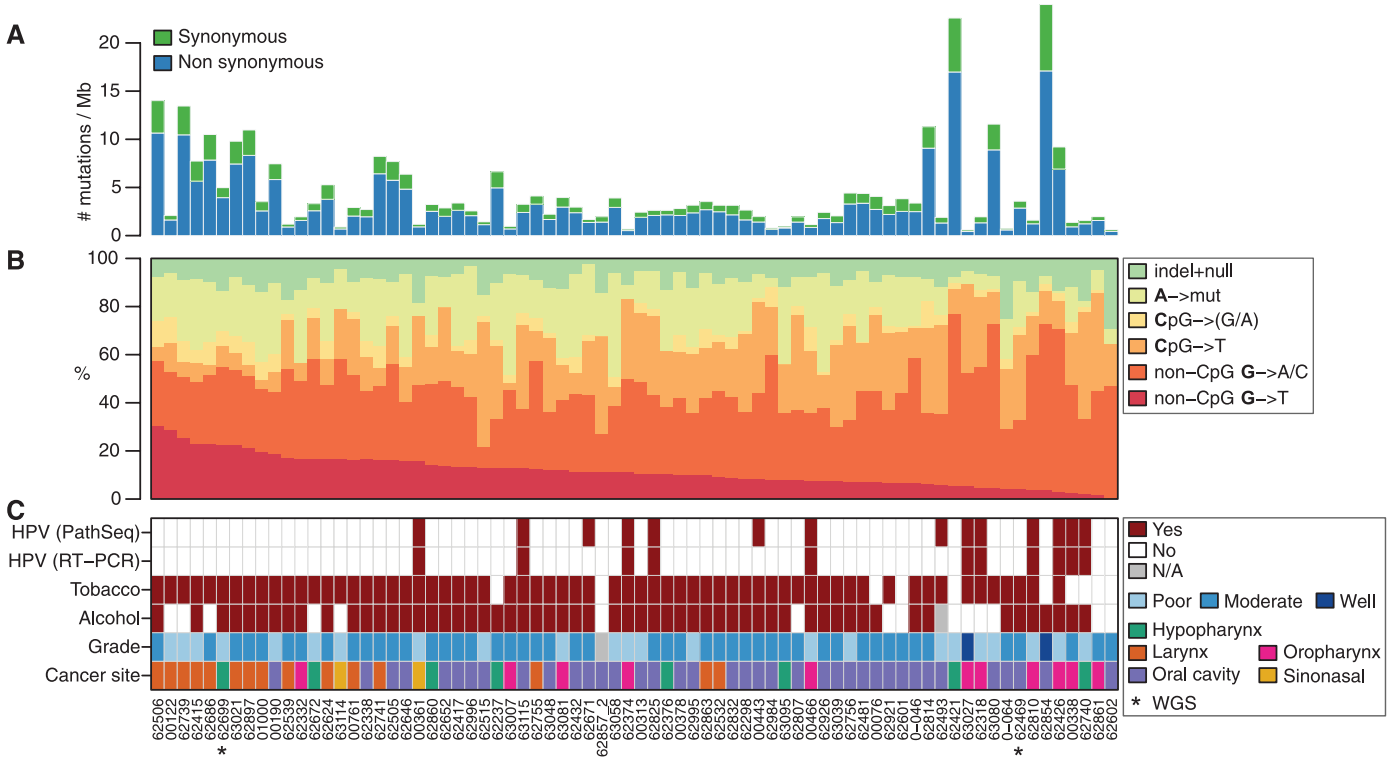

Fig. 1. Mutation rates and base-substitution frequencies in head and neck cancers. (**A**) Rate of synonymous and nonsynonymous mutations, expressed in number of mutations per megabase (Mb) of covered target sequence. Nonsynonymous mutation rates range from 0.43 to 17.1 mutations per megabase (mean = 3.3). (**B**) Breakdown of individual base-substitution rates used for statistical significance of mutation recurrence, for the same samples as in (A). The samples were ordered by the rate of G → T transversions, which are indicative of smoking-induced mutations. (**C**) Key clinical parameters for the samples described in (A) and (B) (table S10). The first row indicates HPV detection by sequencing; the second row indicates HPV detection by real-time PCR (RT-PCR). WGS, whole-genome shotgun sequencing.

may represent a robust readout of "functional" tobacco exposure. We observed differences in mutation rates and G → T transversion frequencies by tumor site even when restricting the analysis to HPV-negative tumors. In particular, HPV-negative laryngeal cancers exhibited higher mutation rates and G → T transversion frequencies compared with HPV-negative cancers found in the oral cavity, oropharynx, hypoharynx, or sinonasal cavity ($P = 0.008$ and $P < 0.0001$, respectively, rank sum tests) (Fig. 1, A to C, and fig. S8).

Notwithstanding the overall apparent correlation between G → T transversions and mutation rates, several "outlier" tumors showed elevated mutation rates, despite a low fraction of G → T transversions. Some of these tumors contained mutations in one or more DNA repair genes. Notably, both HNSCC tumors with the highest mutation rates occurred in nonsmokers (Fig. 1). These results raise the possibility that some HNSCC tumors may contain genetic alterations that promote elevated mutation rates apart from the effects of tobacco (supporting online material).

To explore the biological basis of HNSCC in an unbiased manner, we used the MutSig algorithm (*7*) to identify genes harboring more mutations than expected by chance, given the total number of mutations detected. This analysis revealed 39 genes with high statistical significance of mutations (false discovery rate $q < 0.1$) (figs. S6 and S7 and tables S6 and S7). Compared with recent cancer

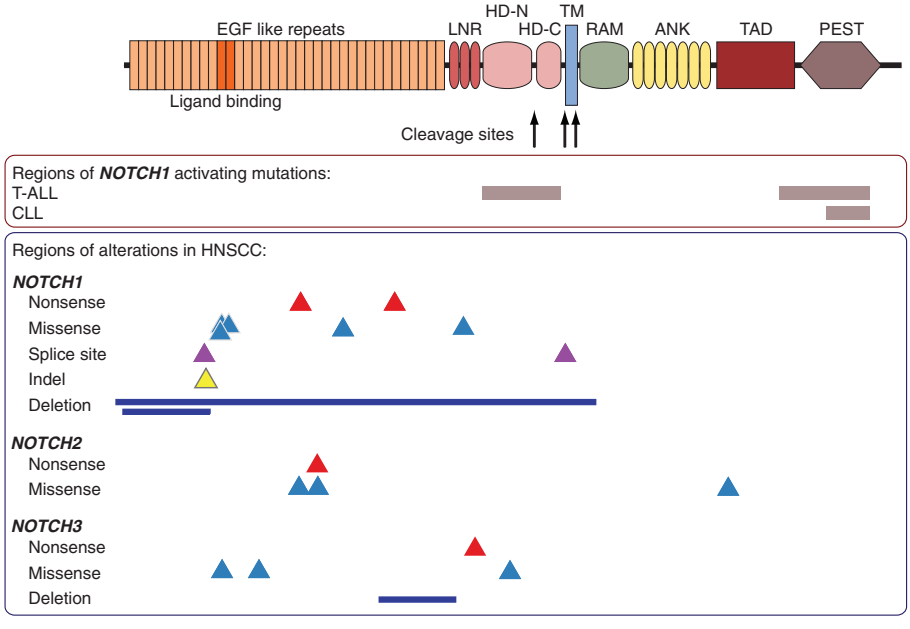

Fig. 2. NOTCH gene mutations identified in head and neck cancer. (**Top**) Schematic diagram of the domain structure of *NOTCH1* (domain structures of *NOTCH2* and *NOTCH3* are similar). (**Middle** and **Bottom**) NOTCH genetic alterations in T-ALL, CLL, and HNSCC. All nonsense mutations occur upstream of the transcriptional activation domain (TAD), which is required for transactivation of target genes. Each arrowhead represents a single point mutation in an individual tumor of the class indicated to the left. EGF, epidermal growth factor; LNR, Lin-12 NOTCH repeats; HD-N, N-terminal heterodimerization domain; HD-C, C-terminal heterodimerization domain; TM, transmembrane; RAM, RBP-Jκ–associated module; ANK, ankyrin repeats; PEST, Pro-Glu-Ser-Thr degradation motif.

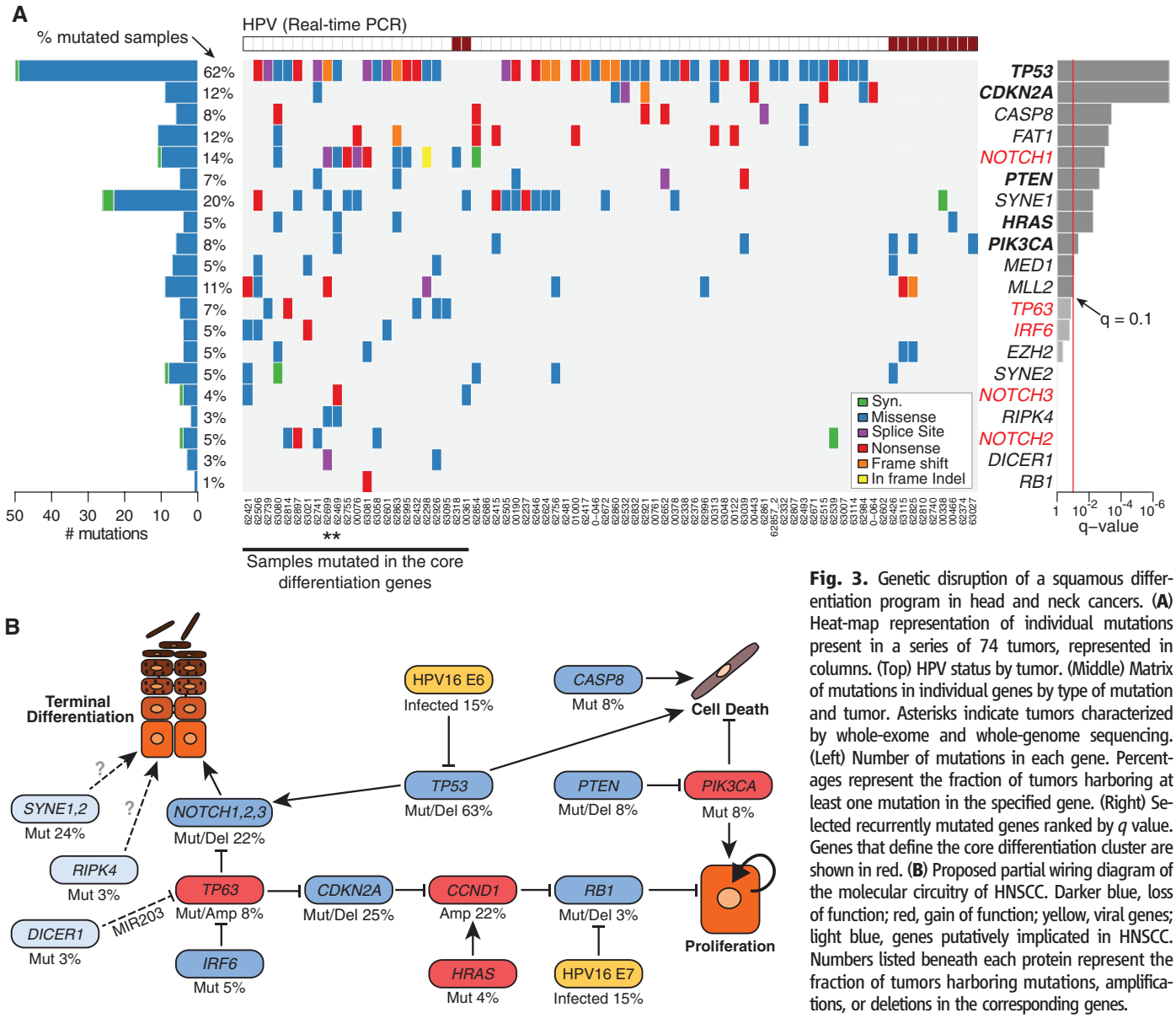

Fig. 3. Genetic disruption of a squamous differentiation program in head and neck cancers. (**A**) Heat-map representation of individual mutations present in a series of 74 tumors, represented in columns. (Top) HPV status by tumor. (Middle) Matrix of mutations in individual genes by type of mutation and tumor. Asterisks indicate tumors characterized by whole-exome and whole-genome sequencing. (Left) Number of mutations in each gene. Percentages represent the fraction of tumors harboring at least one mutation in the specified gene. (Right) Selected recurrently mutated genes ranked by *q* value. Genes that define the core differentiation cluster are shown in red. (**B**) Proposed partial wiring diagram of the molecular circuitry of HNSCC. Darker blue, loss of function; red, gain of function; yellow, viral genes; light blue, genes putatively implicated in HNSCC. Numbers listed beneath each protein represent the fraction of tumors harboring mutations, amplifications, or deletions in the corresponding genes.

genome projects such as those dealing with ovarian cancer and multiple myeloma (*7*, *8*), our analysis of HNSCC revealed a larger number of significantly mutated genes. However, the majority of mutated genes did not reach statistical significance (table S6), suggesting that many may contain passenger events. Thus, we hypothesized that the MutSig algorithm identified an enriched set of genes that probably underwent positive selection during tumorigenesis. Toward this end, numerous significantly mutated genes had previously been implicated in HNSCC—including *TP53*, *CDKN2A*, *HRAS*, *PTEN*, and *PIK3CA* ($q < 0.1$) (*4*)—providing support for the validity of the approach. *TP53*, the most commonly mutated gene in HNSCC, was also disrupted by a 100-kb deletion detected by whole-genome sequencing and validated with a focal copy-number change detected by SNP array (fig. S9). However, most significantly mutated genes had not previously been implicated in HNSCC.

To explore their biological importance, we first considered mutated HNSCC genes that also undergo frequent genetic alterations in other cancers. *NOTCH1* was particularly noteworthy: Point mutations affecting this gene occurred in 11% of the HNSCC tumors (Figs. 2 and 3 and tables S6 and S7), and focal deletions were seen in two additional tumors (Fig. 2). Previous evidence from animal models had implicated Notch dysregulation in cutaneous squamous cell carcinoma (*9*), but somatic *NOTCH1* mutations had not previously been identified in squamous malignancies. In addition, we found nonsynonymous point mutations in *NOTCH2* or *NOTCH3* in 11% of the samples (Figs. 2 and 3 and table S6) and a focal deletion of *NOTCH3* in one additional case (Fig. 2). Whereas *NOTCH1* contains activating mutations in T cell acute lymphoblastic leukemia and chronic lymphocytic leukemia (*10*, *11*) and *NOTCH2* contains activating mutations in diffuse large B cell lymphoma (*12*), the mutations in HNSCC appeared to be loss-of-function mutations, consistent with those recently described for myeloid leukemia (*13*).

Several *NOTCH1* nonsense mutations in HNSCC are predicted to generate truncated proteins that lack the C-terminal ankyrin repeat domain, a region critical for transactivation of target genes (Fig. 2) (*14*). Five additional mutations (four missense and one in-frame deletion) cluster in highly conserved residues situated within or nearby the extracellular ligand binding domain (Fig. 2). Two others are splice-site mutations that may generate truncated proteins or delete critical functional residues (for instance, ligand binding or activation by proteolytic cleavage) (Fig. 2). Together, these findings suggested that NOTCH dysregulation—and, more generally, mechanisms governed by NOTCH signaling—contribute to the genesis or progression of HNSCC.

To further interpret the mutations identified in HNSCC, we looked for functionally related gene sets harboring an excess of mutations. For this purpose, we considered an expanded list of 76 genes ($q < 0.25$) (table S7) and looked for enrichment in functional gene sets. The highest-scoring gene set contained genes related to epidermal development (table S8). The significantly mutated genes ($q < 0.25$) in this set included *NOTCH1*, *IRF6*, and *TP63*. These genes are all clearly related to squamous differentiation. The most abundant *TP63* protein product in squamous epithelia, known as ΔNp63, promotes renewal of basal keratinocytes by a mechanism that requires down-regulation of *NOTCH1* and *CDKN2A* (*15*–*17*). IRF6, in turn, has been implicated in the proteasomal degradation of ΔNp63 (*18*). Furthermore, terminal differentiation in squamous epithelia is induced in response to genotoxic stress by a mechanism involving p53-dependent transactivation of *NOTCH1*, an activity antagonized by ΔNp63 (*19*). Because HNSCC involves transformation of the squamous epithelial lineage, which is histologically similar to the epidermis, these findings led us to hypothesize that mutations in such genes disrupt a stratified squamous development/differentiation program in precursor cells of this malignancy.

Further inspection of recurrent mutations identified 11 additional genes carrying disruptive mutations that function in the squamous differentiation program. The evidence includes mouse knockouts with defects in squamous epithelial differentiation (*Notch1*, *Notch2*, *Irf6*, *Tp63*, *Ripk4*, *Cdh1*, *Ezh2*, and *Dicer1*) (Fig. 3A) (*20*–*25*), human germline mutations causing orofacial clefting syndromes (*IRF6*, *TP63*, *CDH1*, and *MLL2*) (*26*), and knockdown or deregulated expression leading to a differentiation block and increased proliferation in cultured human keratinocytes (*TP63*, *NOTCH1*, *IRF6*, *MED1*) (*15*, *27*). Thus, many mutated genes in HNSCC may govern squamous differentiation. These mutations may promote an immature and more proliferative basal-like phenotype, consistent with known stages of progression and markers of differentiation in HNSCC (Fig. 3B).

We also found recurrent mutations in less well-characterized genes. For example, we observed mutations in *SYNE1* and *SYNE2* in 20 and 8% of HNSCC samples, respectively (fig. S7 and tables S6 and S7). These genes have been implicated in the regulation of nuclear polarity (*28*), a process that operates upstream of NOTCH1 in squamous epithelia (Fig. 3B) (*29*). *RIMS2* and *PCLO* mutations were seen in 11 and 12% of cases, respectively; the corresponding proteins mediate calcium sensing (*30*), another crucial process for terminal squamous differentiation (*20*).

Beyond the genes directly involved in squamous differentiation, we found mutations involving two apoptosis-related genes: *CASP8* (8%) and *DDX3X* (4%) (fig. S7 and table S7). Thus, suppression of apoptosis may also contribute to HNSCC pathogenesis, perhaps in concert with disrupted squamous maturation (Fig. 3B). The histone methyltransferases *PRDM9* (11%) and *EZH2* (6%) are also recurrently mutated.

Viral infection by HPV figures prominently into the etiology of a subset of HNSCC and is most frequently detected by in situ hybridization or p16 immunohistochemistry. We reasoned that HNSCC genome sequencing might also offer a robust HPV detection method. We therefore used the PathSeq algorithm (*31*) and a viral sequence database to identify HNSCC sequencing reads that aligned to HPV genomes. We observed HPV-16 sequence reads in 14 tumors (19%) (range: 1 to 40,000 reads), 11 of which were also positive by HPV-16 PCR ($P < 0.0001$) (table S9). The three tumors that were HPV-negative by PCR had very low HPV-16 sequence read counts (fig. S10); this may reflect reduced HPV dosage or technical contamination. We observed an inverse correlation between HPV status (determined by sequencing) and *TP53* mutation, as shown previously ($P = 0.001$, Fisher's exact test) (*32*). These data underscore the potential utility of massively parallel sequencing to detect both human and nonhuman etiologic agents in tumor specimens.

Given that NOTCH pathway inhibitors have entered clinical trials, the discovery of loss-of-function *NOTCH1* mutations in HNSCC may have important therapeutic implications. A recent clinical trial of a γ-secretase inhibitor (which inhibits NOTCH) was halted in part because of an increased frequency of skin cancers in the treatment arm (*33*). This clinical observation is consistent with those from mouse models, in which cutaneous knockout of *Notch1* promotes skin tumor formation (*24*). Our results suggest that patients taking γ-secretase inhibitors may require monitoring for the development of both cutaneous and head/neck squamous malignancies.

Despite the anatomical distinctions that dominate current clinical management of HNSCC, our results point to several unifying features at the molecular level. For example, *TP53* inactivation, either through somatic mutation or HPV infection, appears nearly universal in this malignancy. The present study suggests that disruption of the squamous differentiation program may represent an additional overarching feature that occurs by numerous genetic mechanisms across tumors from multiple anatomic sites. Thus, HNSCC pathogenesis may involve a maturation arrest or a lineage dependency similar to that seen in other cancer types (*34*). However, HNSCC appears to be unusual in that the mutational etiology is diverse, in contrast to leukemia and prostate cancer in which developmental pathologies appear to be caused by lesions in only a few target genes. Rational therapeutic avenues targeting this block in squamous differentiation may require synthetic lethal approaches to identify specific cellular dependencies arising from NOTCH inactivation, TP63 alteration, or other events that deregulate the program. Finally, our results demonstrate that whole-exome sequencing of large numbers of tumor/normal pairs should enable fundamental new insights into tumor biology that are relevant to many human cancers.

References and Notes

1. J. Ferlay *et al.*, *Int. J. Cancer* **127**, 2893 (2010).
2. A. Argiris, M. V. Karamouzis, D. Raben, R. L. Ferris, *Lancet* **371**, 1695 (2008).
3. S. Gupta, W. Kong, Y. Peng, Q. Miao, W. J. Mackillop, *Int. J. Cancer* **125**, 2159 (2009).
4. C. R. Leemans, B. J. Braakhuis, R. H. Brakenhoff, *Nat. Rev. Cancer* **11**, 9 (2011).
5. W. Lee *et al.*, *Nature* **465**, 473 (2010).
6. E. D. Pleasance *et al.*, *Nature* **463**, 184 (2010).
7. M. A. Chapman *et al.*, *Nature* **471**, 467 (2011).
8. The Cancer Genome Atlas Research Network, *Nature* **474**, 609 (2011).
9. U. Koch, F. Radtke, *Curr. Top. Dev. Biol.* **92**, 411 (2010).
10. X. S. Puente *et al.*, *Nature* **475**, 101 (2011).
11. J. C. Sok *et al.*, *Clin. Cancer Res.* **12**, 5064 (2006).
12. S. Y. Lee *et al.*, *Cancer Sci.* **100**, 920 (2009).
13. A. Klinakis *et al.*, *Nature* **473**, 230 (2011).
14. R. A. Kovall, S. C. Blacklow, *Curr. Top. Dev. Biol.* **92**, 31 (2010).
15. B. C. Nguyen *et al.*, *Genes Dev.* **20**, 1028 (2006).
16. R. Okuyama *et al.*, *Oncogene* **26**, 4478 (2007).
17. X. Su *et al.*, *EMBO J.* **28**, 1904 (2009).
18. F. Moretti *et al.*, *J. Clin. Invest.* **120**, 1570 (2010).
19. T. Yugawa *et al.*, *Cancer Res.* **70**, 4034 (2010).
20. C. Blanpain, E. Fuchs, *Nat. Rev. Mol. Cell Biol.* **10**, 207 (2009).
21. M. Chidgey *et al.*, *J. Cell Biol.* **155**, 821 (2001).
22. A. Dumortier *et al.*, *PLoS ONE* **5**, e9258 (2010).
23. E. Ezhkova *et al.*, *Genes Dev.* **25**, 485 (2011).
24. M. Nicolas *et al.*, *Nat. Genet.* **33**, 416 (2003).
25. C. L. Tinkle, T. Lechler, H. A. Pasolli, E. Fuchs, *Proc. Natl. Acad. Sci. U.S.A.* **101**, 552 (2004).
26. Online Mendelian Inheritance in Man, www.ncbi.nlm.nih.gov.
27. C. L. Tu, W. Chang, Z. Xie, D. D. Bikle, *J. Biol. Chem.* **283**, 3519 (2008).
28. Y. Lüke *et al.*, *J. Cell Sci.* **121**, 1887 (2008).
29. S. E. Williams, S. Beronja, H. A. Pasolli, E. Fuchs, *Nature* **470**, 353 (2011).
30. K. Fujimoto *et al.*, *J. Biol. Chem.* **277**, 50497 (2002).
31. A. D. Kostic *et al.*, *Nat. Biotechnol.* **29**, 393 (2011).
32. W. H. Westra *et al.*, *Clin. Cancer Res.* **14**, 366 (2008).
33. A. Extance, *Nat. Rev. Drug Discov.* **9**, 749 (2010).
34. L. A. Garraway, W. R. Sellers, *Nat. Rev. Cancer* **6**, 593 (2006).

Acknowledgments: We thank the Broad Institute Sequencing Platform for the generation of sequencing data, the staff of the Biological Samples Platform and the Genetic Analysis Platform at the Broad Institute, and J. Aster for helpful discussions. This work was conducted as part of the Slim Initiative for Genomic Medicine, a joint U.S.-Mexico project funded by the Carlos Slim Health Institute, and is part of a global effort in collaboration with the International Cancer Genome Consortium. The work was also supported by grants from the National Human Genome Research Institute (S.B.G., E.S.L.), the National Cancer Institute (M.M., S.B.G., L.A.G., J.R.G., A.M.E.), the Starr Cancer Consortium (L.A.G.), the Novartis Institutes for BioMedical Research (N.S.), the Howard Hughes Medical Institute (T.R.G.), the American Cancer Society (J.R.G.), and the NIH Director's New Innovator Award (L.A.G.). L.A.G. and M.M. are paid consultants for and equity holders in Foundation Medicine, a genomics-based oncology diagnostics company, and are also paid consultants for Novartis. M.F.B. is a paid consultant for Foundation Medicine. E.S.L. is an equity holder in Foundation Medicine. The compressed binary Sequence Alignment/Map files (BAM) and SNP array data are available in dbGaP under accession no. phs000370.v1.p1.

Supporting Online Material

www.sciencemag.org/cgi/content/full/science.1208130/DC1
Materials and Methods
SOM Text
Figs. S1 to S10
Tables S1 to S11
References (*35*–*66*)

10 May 2011; accepted 5 July 2011
Published online 28 July 2011;
10.1126/science.1208130